GEOLOGY | THE GEOLOGICAL SOCIETY OF AMERICA®

https://doi.org/10.1130/G51671.1

Manuscript received 22 August 2023
Revised manuscript received 5 October 2023
Manuscript accepted 17 October 2023

Published online 30 October 2023

Effect of short-term, climate-driven sediment deposition on tectonically controlled alluvial channel incision

Xueliang Wang[1,2,*], John J. Clague[3], Paolo Frattini[4], Shengwen Qi[1,2], Hengxing Lan[5], Wen Zhang[6], Lihui Li[1,2], Juanjuan Sun[1,2], and Giovanni Battista Crosta[4]

[1]Key Laboratory of Shale Gas and Geoengineering, Institute of Geology and Geophysics, Chinese Academy of Sciences, Beijing 100029, China
[2]College of Earth and Planetary Sciences, University of Chinese Academy of Sciences, Beijing 100049, China
[3]Department of Earth Sciences, Simon Fraser University, Burnaby, British Columbia V5A 1S6, Canada
[4]Department of Earth and Environmental Sciences, Università degli Studi di Milano-Bicocca, Piazza della Scienza 4, Milano 20126, Italy
[5]State Key Laboratory of Resources and Environmental Information System, Institute of Geographic Sciences and Natural Resources Research, Chinese Academy of Sciences, Beijing 100101, China
[6]College of Construction Engineering, Jilin University, Changchun 130026, China

ABSTRACT

Debate about relations between rates of fluvial incision and time (the "Sadler effect") continues, impeding the use of incision rates to infer tectonic and climatic processes. There is a dearth of detailed field evidence that can be used to explore the coupling between tectonics and climate in controlling alluvial channel geometry and incision rates over time scales of 10^2–10^5 yr. We present field data from the Rumei watershed of southeast Tibet, which we obtained by mapping and dating late Pleistocene (ca. 135 ka) fluvial terraces and related channels, measuring channel hydraulic geometry, and calculating channel steepness indexes and incision rates. The evidence indicates that climate forcing is the main driver of sediment production and delivery to streams in the watershed. New aggradation events altered alluvial valley and channel geometry and, coupled with tectonic uplift, affected the rate of channel incision in the catchment. We propose a conceptual model $\left(I_1 - \frac{\sum_1^n h_{i(t)}}{T}\right)$ that links uplift-driven incision (I_1) to channel aggradation $\left(\frac{\sum_1^n h_{i(t)}}{T}\right)$ induced by climate change, which is valid in catchments and other areas. We conclude that the reduction in incision depth caused by climate-driven channel aggradation is significant on short time scales (10^2–10^5 yr), and its cumulative effect contributes to the "Sadler effect" on long time scales (>10^6 yr).

INTRODUCTION

Incision rates derived from measurements of channel geometry and dating of geological or geomorphic markers are widely used to calculate rock uplift rates and infer the effect of climate change (Burbank et al., 1996; Finnegan et al., 2005; Malatesta et al., 2018). Sadler (1981) showed that rates of sediment accumulation in stratigraphic sequences have an inverse relation to the measurement interval (the "Sadler effect"; Schumer and Jerolmack, 2009). It follows, and has been shown, that incision rates calculated from the elevation difference between dated river terraces and the modern riverbed also exhibit a negative power-law dependence on the measured time interval (Mills, 2000; Finnegan et al., 2014). In some literature, this relation has also been referred to as the "Sadler effect" (Gallen et al., 2015; Nativ and Turowski, 2020). The "Sadler effect" implies that conclusions based on comparisons of incision rates calculated over different time intervals may be misleading (Gardner et al., 1987).

Finnegan et al. (2014) documented the negative power-law dependence of incision rates on measurement interval over 10^4–10^7 yr globally and attributed this time dependency to episodic hiatuses (Jerolmack and Paola, 2010). In contrast, Gallen et al. (2015) questioned the necessity of invoking hiatuses to explain this effect and rather argued that it is the result of a systematic bias related to modern streambed elevation variability. However, the validity of measurement bias to explain the "Sadler effect" (Gallen et al., 2015) was questioned by Nativ and Turowski (2020), who showed a site-specific dependence of incision on time scale. Malatesta et al. (2017) commented further on this debate by highlighting the importance of considering fill and fill-cut terraces when calculating incision rates, rather than using only records of strath terraces. Overall, the "Sadler effect" is still being investigated and debated.

Although some studies have provided important information on individual alluvial terraces that bear on ideas about channel evolution (Ouimet et al., 2009; Malatesta et al., 2017), few studies have systematically investigated sets of landforms and sediments in a single high-mountain catchment to explore the evolution of alluvial channel geometry and incision rates controlled by climate and tectonics (Lavé and Avouac, 2001; Dey et al., 2016; Zhang et al., 2021). Lavé and Avouac (2001) used fluvial incision rates calculated from terraces to show that river incision across the Himalayas of central Nepal is balanced over the long term by tectonic uplift. Dey et al. (2016), on the other hand, showed that cycles of aggradation and river incision were driven by climatic forcing in the Kangra Basin of the northwest Sub-Himalaya,

Xueliang Wang https://orcid.org/0000-0002-0937-5605
*wangxueliang@mail.iggcas.ac.cn

CITATION: Wang, X., et al., 2024, Effect of short-term, climate-driven sediment deposition on tectonically controlled alluvial channel incision: Geology, v. 52, p. 17–21, https://doi.org/10.1130/G51671.1

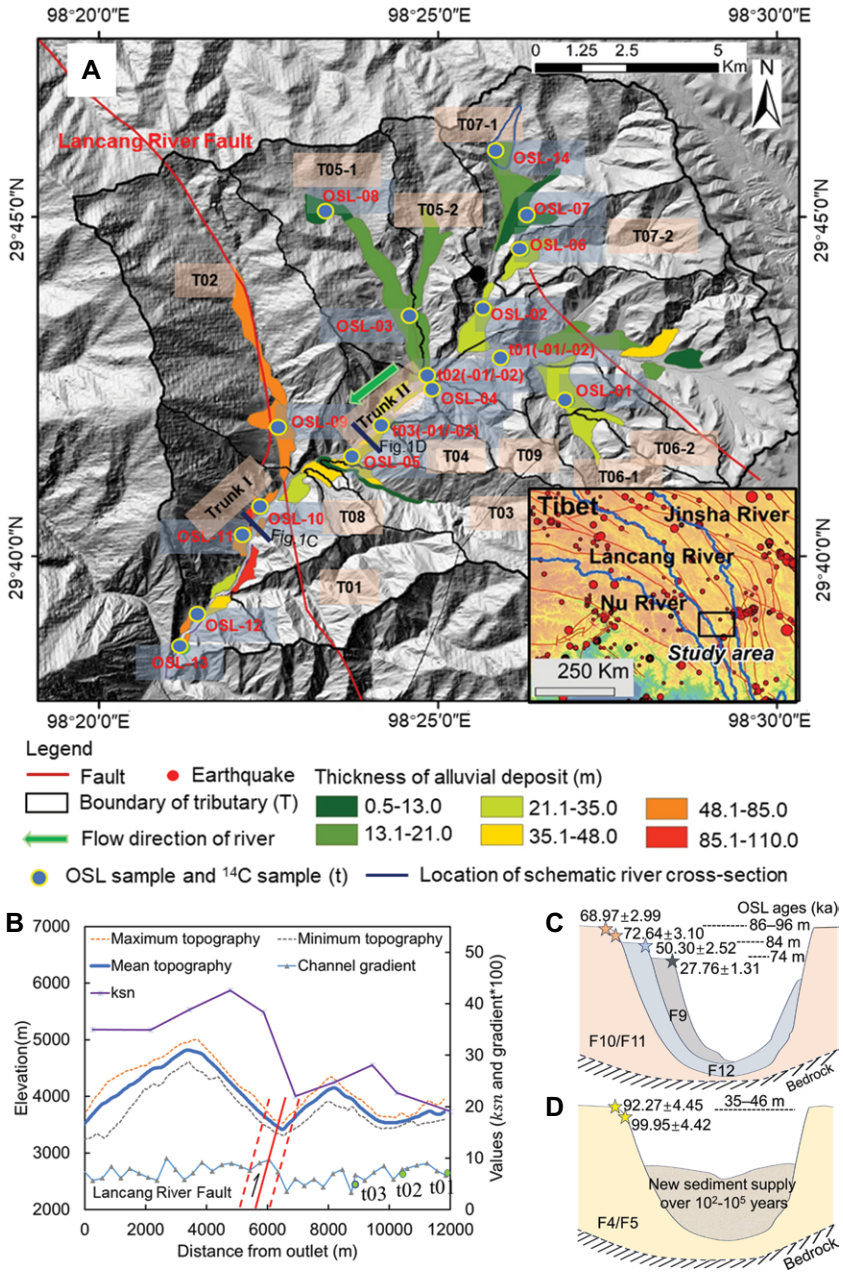

Figure 1. (A) Distribution of terraces in Rumei catchment and locations of samples that were collected to date terraces. Inset map shows location of study area (black rectangle). OSL—optically stimulated luminescence. (B) Topographic elevation, channel gradient, and normalized river steepness (k_{sn}) as function of distance along river. (C) Schematic river cross section showing major episodes of aggradation related to downstream (F9–F11) terraces (see Fig. S2 [see text footnote 1]). (D) Schematic cross section through F4–F5 terraces.

and Zhang et al. (2021) related the spatial pattern of fluvial incision along the Lancang River in southeast Tibet to contemporary tectonics.

We selected the Rumei catchment (RMC) in the mountains of southeast Tibet (Fig. 1) to address questions related to the spatiotemporal patterns of climate-driven sediment production and delivery to streams and the spatial variation and evolution of coupled tectonic-climate–controlled alluvial channel geometry and river incision rates over 10^2–10^5 yr. We present evidence bearing on the following questions: When did sediment supply and terrace abandonment occur in the watershed? How does the interplay of climate and tectonic drivers produce the "Sadler effect"?

MATERIALS AND RESULTS

The RMC is a 181 km^2 watershed located between E-W–trending thrust faults and dextral strike-slip faults in the mountains of southeast Tibet. The watershed is bounded by the Lancang River fault (LCRF), which is a major active structure with an average slip rate near the RMC of ~3.5 + 1.1/–0.8 mm/yr (Ren et al., 2022). The LCRF is thought to be have formed between ca. 5.9 and 3.9 Ma (Ren et al., 2022), and it remains active today (Guo et al., 2000).

Ages of Fluvial Terraces

Incision rates derived from fluvial fill terraces most reliably record long-term incision rates (e.g., driven by tectonic uplift; Malatesta et al., 2017); thus, our focus here is on fill terraces. Times of fluvial terrace abandonment were based on ages derived from 14 optically stimulated luminescence (OSL) samples (Fig. 1) collected as close as possible to the top of alluvium on terrace treads (see Table S1 and Methods S1–S3 in the Supplemental Material[1]). OSL ages of six samples (OSL-01 to OSL-06) from upstream sites demonstrated that the highest upstream terrace began to develop as a discrete incised surface around 100 ± 10 k.y. ago; a lower one formed around 50 ka. Samples OSL-10 to OSL-12 from sediments covering high terraces at downstream sites demonstrated that the downstream terraces formed between ca. 72 and 50 ka.

We obtained radiocarbon ages ranging from 9270 to 630 cal yr B.P. (Table S2) on six samples of peat collected ~0.8–1.6 m above the level of modern streams to constrain the time of establishment of the modern channel floor (Fig. 1; Supplemental Material).

River Incision Rates and Channel Geometry

Incision rates calculated for 16 terraces ranged from 0.15 to 1.67 mm/yr and were separated into two groups: one group with values larger than 1.0 mm/yr (1.03 ± 0.13 to 1.67 ± 0.24) downstream of the LCRF, and a second group with values <0.6 mm/yr (0.15 ± 0.03 to 0.58 ± 0.07) upstream of the fault (Fig. S3). The average incision rate of the first group (1.37 ± 0.26 mm/yr) is more than four times that of the second group (0.30 ± 0.15 mm/yr).

Researchers have documented differences in river gradient and channel width where rivers cross active normal and thrust faults (Lavé and Avouac, 2001). Along the trunk river, the channel gradient downstream of the LCRF is twice that of the upstream side (Fig. 1B). The river also has a narrower channel downstream of the LCRF than upstream of the fault (Fig. 2A). Based on the longitudinal profile of the trunk stream, values of normalized river steepness, denoted k_{sn} (Fig. 1B; Supplemental Material), were also divided into two groups, a group with values <27 upstream of the LCRF and a second group with values ranging from 27 to 43 downstream of the fault.

[1]Supplemental Material. Methods S1–S3; Figures S1–S6; and Tables S1–S2. Please visit https://doi.org/10.1130/GEOL.S.24328717 to access the supplemental material; contact editing@geosociety.org with any questions.

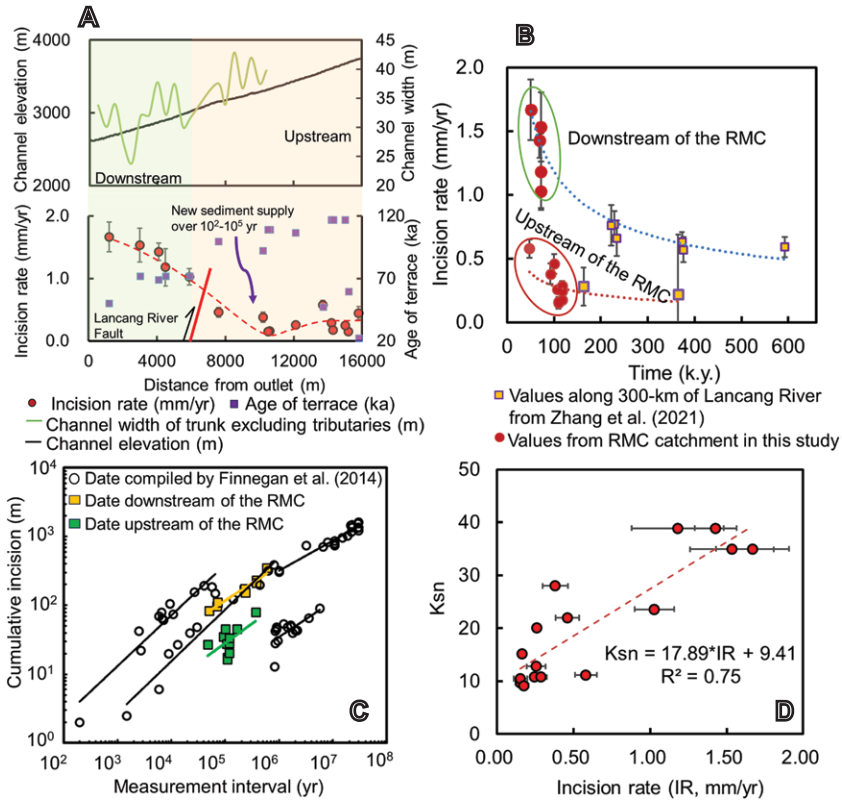

Figure 2. (A) Plots of ages of terraces (ka), calculated incision rates, and channel elevation and channel width as function of distance along trunk river. (B) Measured incision rate as function of time. (C) Log-log plot of cumulative alluvial incision vs. time interval for data set displaced in B and data from Finnegan et al. (2014). (D) Plot of incision rate vs. normalized channel steepness (k_{sn}) in Rumei catchment (RMC).

DISCUSSION

Effect of Climate on Aggradation

There is a correspondence between marine oxygen isotope stages (MISs) and glaciation in Tibet (Wang et al., 2008), and so we used MISs (Raymo, 1997) as proxies for glaciation in the Rumei watershed. Fluvial deposits upstream of the LCRF and associated with terraces F1–F5 had a total volume of ~0.16 km^3 and formed during MIS 5. Renewed aggradation of trunk I, with sediment totaling ~0.10 km^3 in volume and sourced from tributary 02, occurred later near the transition from MIS 5 to MIS 4 (72.64 ± 3.10 ka; Fig. 3A). Two terraces formed during MIS 3, which was a period thought to have been warmer than either MIS 4 or MIS 2.

We hypothesized that there would be elevated sediment delivery from the headwaters of the RMC during Pleistocene glacial stages due to glacial and periglacial processes at those times. The elevated sediment flux (Q_S) would then exceed the capacity of the trunk stream (Q_w) to transport the sediment out of the system (Fig. 3B). In contrast, during relatively warm and humid interglacials and interstadials, significant increases in Q_w would lead to episodic aggradation and transport along the trunk and tributary streams (Malatesta and Avouac, 2018). The transition from glacial to interglacial periods, marked by aggradation and subsequent incision of valley fills in the RMC, accords with the classic paraglacial cycle of Church and Ryder (1972).

Changes in Incision Rates Due to Aggradation Events

Calculated incision rates associated with sequential sediment delivery events differed by only small amounts over a reach distance of ~5 km along the upstream trunk channel (0.15 ± 0.04 − 0.46 ± 0.08 mm/yr). However, calculated incision rates were several times these values along the downstream trunk channel, with a tendency toward an increase in the downstream direction (Fig. 2A). Sediments derived from upstream sources over the past 9300 yr have been carried through the lower part of the watershed without aggrading the trunk channel downstream of the LCRF due to faster uplift and incision in that area. Upstream reaches, however, have been more profoundly affected by these sediment pulses. Hence, we attribute differences in calculated incision rates (Fig. 2A), in part, to the episodic delivery of large amounts of new sediment to tributary and trunk streams.

Conceptual Model

Taking into account previously published rates along an ~300-km-long reach of the Langcang River (Zhang et al., 2021), we found that incision rates both within and downstream of the RMC showed a negative power-law dependence on the time interval considered (Fig. 2B). In our study, values of the scaling exponent of cumulative incision versus the measurement interval for periods of 10^4–10^6 yr were 0.51–0.57, comparable with those of Finnegan et al. (2014) over 10^4–10^7 yr (Fig. 2C). Hence, we infer that the trend observed here at a single locality is similar to the global trend.

We propose that new sediments deposited on valley floors increase the elevation of the stream channel and hence reduce the measured incision depth between the modern streambed and older relict dated terraces (D_{MT}; Fig. 4A; Fig. S4). The reduction in incision depth due to each aggradation event ($h'_{i(t)}$; Fig. 4A) is related to Q_S and Q_w, which in turn are strongly influenced by climate. In general, increases in precipitation convey more sediment to river channels (Dey et al., 2016), resulting in larger $h'_{i(t)}$ and their summed values than those of a cold climate with low precipitation. The difference between the recovered initial incision depth and an assumed depth reached under presumptively undisturbed initial conditions (sum of $h_{i(t)}$; Fig. 4A) is a measure of the relative effects of climate-driven sedimentation and tectonic uplift on channel incision.

Considering the effect of climate-driven alluvial dynamics, the incision rate, I_{MT} (where MT denotes the relation of the modern river to the reference fill terrace), can be estimated as follows:

$$I_{MT} = \frac{D_{MT}}{T} = I_I - \frac{\sum_1^n h_{i(t)}}{T}, \qquad (1)$$

where T is the age of the reference fill terrace, and t is the time of the aggradation event. Older terraces have experienced more climate-driven aggradation events than younger ones in the current MIS stage, leading to larger total reductions in incision depth (H_T). In this case, we can expect a larger reduction in incision rate ($\triangle I_{MT}$; Fig. 4B) for older terraces than younger ones under a condition of $dH_T/dT > 1$. Our proposed conceptual model explains the cumulative effect of climate-driven aggradation events in reducing the background tectonically controlled incision of alluvial terraces. From Equation 1, we observe that the difference in incision rates ($\triangle I_{MT}$) calculated from different periods of terraces is independent of tectonic-controlled incision rate; hence, we infer that the alluvial "Sadler effect" may have little to do with tectonic activity, which is consistent with observation of Finnegan et al. (2014).

Our model also allows us to roughly estimate volumes of sediment that have aggraded alluvial channels on time scales approaching 10^6 yr. Using the model, we can estimate H_T

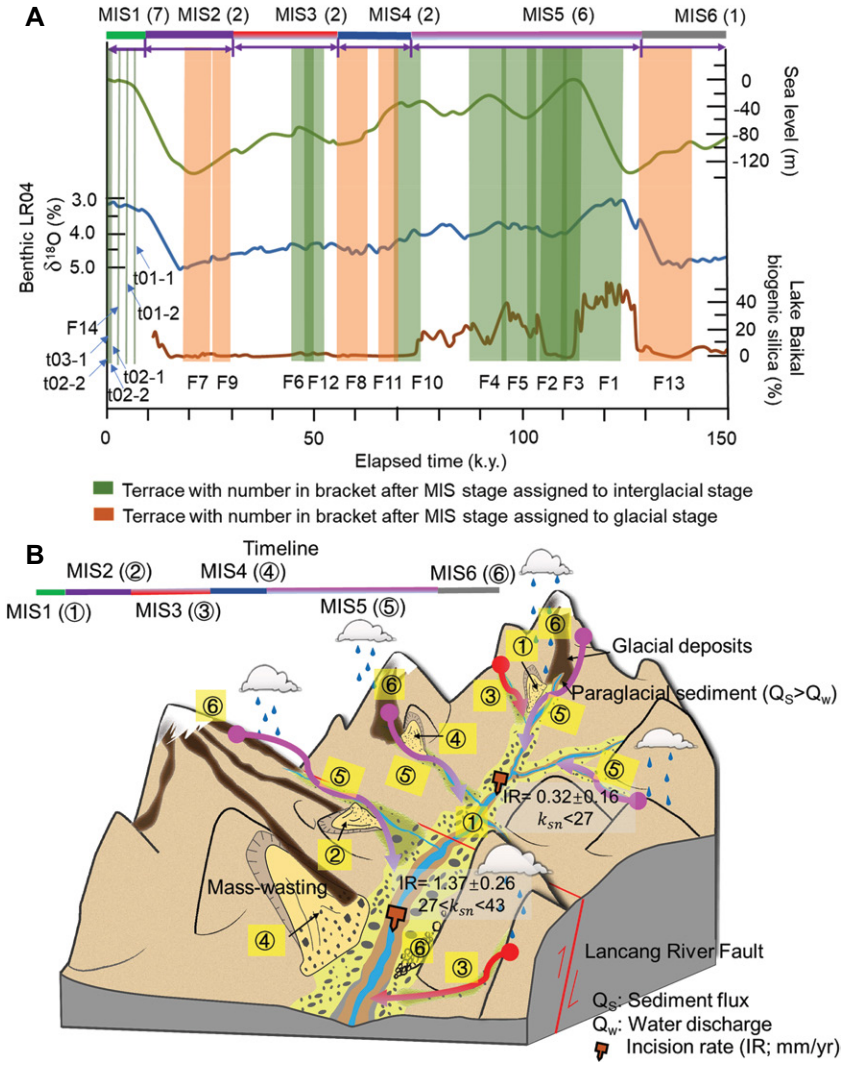

Figure 3. (A) Ages of F1 to F14 fluvial terraces and major sediment transport events. Marine isotope stage (MIS) 1–6 climate proxies include composite sea-level record of Spratt and Lisiecki (2016); benthic LR04 δ^{18}O record (Lisiecki and Raymo, 2005); and Lake Baikal biogenic silica record of Prokopenko et al. (2006). (B) Schematic block diagram illustrating inferred evolution of Rumei catchment in response to climate forcing and uplift over late Pleistocene and Holocene (k_{sn} is normalized channel steepness).

occurring by climatically controlled aggradation over a particular period of time (T) using the following equation:

$$H_T = (I_I - I_{MT})T = (I_I - \alpha T^{\lambda})T, \qquad (2)$$

where α and λ are constants in the relationship between incision rates and terraces ages (e.g., 11.32 and −0.49 in Fig. 2B). As an example application, we can approximately expect the cumulative depth of climate-driven sedimentation as (I_I – 11.32 × 120$^{-0.49}$) × 120 m passing through a terrace formed 120 k.y. ago in the RMC.

Effect of Rock Uplift on Fluvial Incision

Previous studies have shown that bedrock uplift in tectonically active mountain ranges drives fluvial incision (Burbank et al., 1996; Snyder et al., 2000; Val et al., 2018). The relatively low-gradient reach upstream of the LCRF in our study area is characterized by a broad zone of alluvium deposited in shallow channels. Downstream of the LCRF, the channel is steeper, and the floodplain width is narrower, indicating stronger tectonically controlled incision in that area. The river channel and initial incision rate downstream of the RMC are controlled by uplift, which is sufficient to incise the bedrock channel. We expect that sediments deposited in the river channel downstream of the LCRF are ephemeral and are removed over the time scales of interest here due to intense vertical incision and lateral migration (Malatesta et al., 2017) induced by active uplift.

Observations and models of fluvial erosion indicate that there is a positive relationship between the rate of bedrock uplift and k_{sn} (Kirby and Whipple, 2012), and that k_{sn} is a good metric for the channel incision rate (Safran et al., 2005). Our results suggest a good linear fit ($R^2 = 0.75$) between k_{sn} and incision rates in the RMC (Fig. 2D).

The LCRF has been active since at least the late Pleistocene (Guo et al., 2000). Higher incision rates downstream of the fault (1.03–1.67 mm/yr) are consistent with higher k_{sn} values for this reach. We suspect that the LCRF has affected fluvial form and incision in the RMC for as long as it has been active (>10^6 yr; Cyr and Granger, 2008). We conclude that long–time-scale (>10^6 yr) features and processes (river and hillslope gradients and bedrock incision rates) are likely linked primarily to tectonics, whereas short–time-scale (10^2–10^5 yr) features and processes (formation of alluvial terraces and dynamic changes in alluvial incision depth) are more likely linked to climate.

CONCLUSIONS

Differences in alluvial incision rates calculated from elevation differences of dated river terraces and the modern riverbed imply an interplay between tectonics and climate. Rapid rock uplift drives rapid incision, as indicated in this study by higher k_{sn} values, a steeper RMC trunk channel, a narrower channel width, and four times the average rate of river incision downstream of the trace of the LCRF than upstream of the fault. Using a conceptual model, we roughly estimated the volume of sediment passing through the alluvial system and thus erosion of the catchment since the formation of a watershed-wide set of terraces that formed ~10^5 yr ago. Climate-driven sedimentation events intermittently reduce alluvial incision depths on short time scales (10^2–10^5 yr). Their cumulative effect slows the tectonic-controlled incision on long time scales (>10^6 yr), thus contributing to the "Sadler effect" on a catchment scale.

ACKNOWLEDGMENTS

This work was supported by the Second Tibetan Plateau Scientific Expedition and Research Program (2019QZKK0904) and the National Natural Science Foundation of China (42172304, 42041006, and 41941019). We thank editor Rob Strachan, reviewer Luca Malatesta, and one anonymous reviewer, whose constructive comments greatly improved our manuscript.

REFERENCES CITED

Burbank, D.W., Leland, J., Fielding, E., Anderson, R.S., Liu, N., Reid, M.R., and Duncan, C., 1996, Bedrock incision, rock uplift and threshold hillslopes in the northwestern Himalayas: Nature, v. 379, p. 505–510, https://doi.org/10.1038/379505a0.

Church, M., and Ryder, J.M., 1972, Paraglacial sedimentation: A consideration of fluvial processes conditioned by glaciation: Geological Society of America Bulletin, v. 83, p. 3059–3071, https://doi.org/10.1130/0016-7606(1972)83[3059:PSACOF]2.0.CO;2.

Cyr, A.J., and Granger, D.E., 2008, Dynamic equilibrium among erosion, river incision, and coastal uplift in the Northern and Central Apennines, Italy: Geology, v. 36, p. 103–106, https://doi.org/10.1130/G24003A.1.

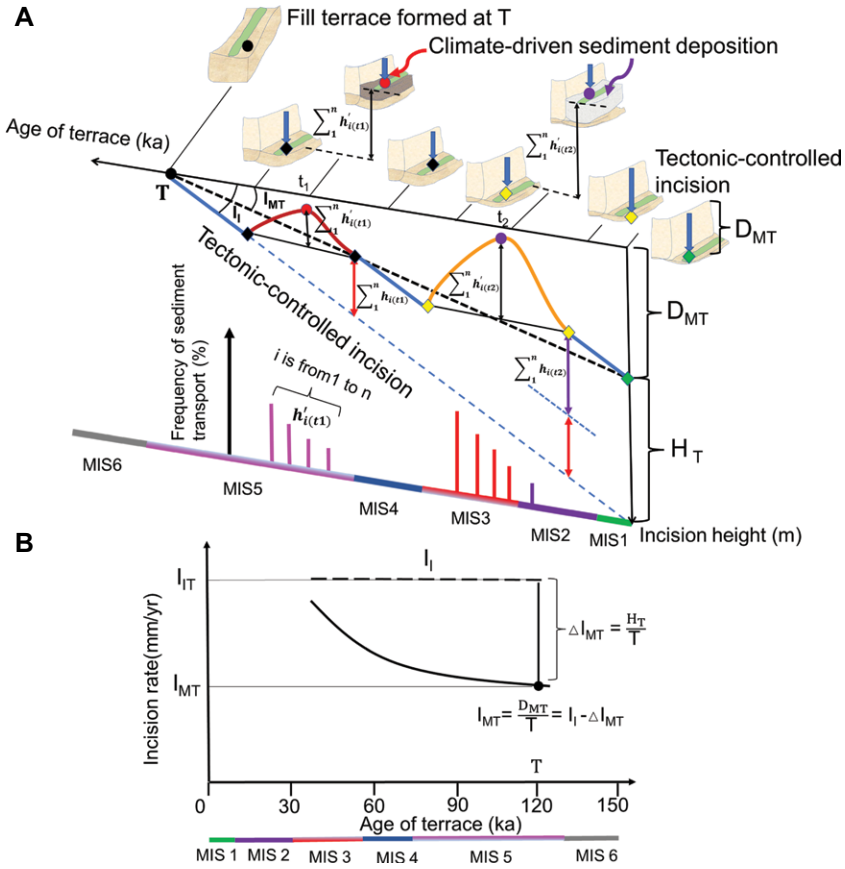

Figure 4. (A) Conceptual model showing that climate-driven channel aggradation events intermittently reduce incision depth. (B) Calculated incision rates depend on length of time over which rate is calculated. MIS—marine isotope stage. See text for definition of variables.

Dey, S., Thiede, R.C., Schildgen, T.F., Wittmann, H., Bookhagen, B., Scherler, D., Jain, V., and Strecker, M.R., 2016, Climate-driven sediment aggradation and incision since the late Pleistocene in the NW Himalaya, India: Earth and Planetary Science Letters, v. 449, p. 321–331, https://doi.org/10.1016/j.epsl.2016.05.050.

Finnegan, N.J., Roe, G., Montgomery, D.R., and Hallet, B., 2005, Controls on the channel width of rivers: Implications for modeling fluvial incision of bedrock: Geology, v. 33, p. 229–232, https://doi.org/10.1130/G21171.1.

Finnegan, N.J., Schumer, R., and Finnegan, S., 2014, A signature of transience in bedrock river incision rates over timescales of 10^4–10^7 years: Nature, v. 505, p. 391–394, https://doi.org/10.1038/nature12913.

Gallen, S.F., Pazzaglia, F.J., Wegmann, K.W., Pederson, J.L., and Gardner, T.W., 2015, The dynamic reference frame of rivers and apparent transience in incision rates: Geology, v. 43, p. 623–626, https://doi.org/10.1130/G36692.1.

Gardner, T.W., Jorgensen, D.W., Shuman, C., and Lemieux, C.R., 1987, Geomorphic and tectonic process rates: Effects of measured time interval: Geology, v. 15, p. 259–261, https://doi.org/10.1130/0091-7613(1987)15<259:GATPRE>2.0.CO;2.

Guo, S., Xiang, H., Zhou, R., Xu, X., Dong, X., and Zhang, W., 2000, Longling-Lancang fault zone in southwest Yunnan, China: Chinese Science Bulletin, v. 45, p. 376–379, https://doi.org/10.1007/BF02909774.

Jerolmack, D.J., and Paola, C., 2010, Shredding of environmental signals by sediment transport: Geophysical Research Letters, v. 37, L19401, https://doi.org/10.1029/2010GL044638.

Kirby, E., and Whipple, K.X., 2012, Expression of active tectonics in erosional landscapes: Journal of Structural Geology, v. 44, p. 54–75, https://doi.org/10.1016/j.jsg.2012.07.009.

Lavé, J., and Avouac, J.P., 2001, Fluvial incision and tectonic uplift across the Himalayas of central Nepal: Journal of Geophysical Research, v. 106, p. 26,561–26,591, https://doi.org/10.1029/2001JB000359.

Lisiecki, L.E., and Raymo, M.E., 2005, A Pliocene–Pleistocene stack of 57 globally distributed benthic $\delta^{18}O$ records: Paleoceanography, v. 20, PA1003, https://doi.org/10.1029/2005PA001164.

Malatesta, L.C., and Avouac, J.P., 2018, Contrasting river incision in north and south Tian Shan piedmonts due to variable glacial imprint in mountain valleys: Geology, v. 46, p. 659–662, https://doi.org/10.1130/G40320.1.

Malatesta, L.C., Prancevic, J.P., and Avouac, J.P., 2017, Autogenic entrenchment patterns and terraces due to coupling with lateral erosion in incising alluvial channels: Journal of Geophysical Research: Earth Surface, v. 122, p. 335–355, https://doi.org/10.1002/2015JF003797.

Malatesta, L.C., Avouac, J.-P., Brown, N.D., Breitenbach, S.F.M., Pan, J., Chevalier, M.-L., Rhodes, E., Saint-Carlier, D., Zhang, W., Charreau, J., Lavé, J., and Blard, P.-H., 2018, Lag and mixing during sediment transfer across the Tian Shan piedmont caused by climate-driven aggradation-incision cycles: Basin Research, v. 30, p. 613–635, https://doi.org/10.1111/bre.12267.

Mills, H.H., 2000, Apparent increasing rates of stream incision in the eastern United States during the late Cenozoic: Geology, v. 28, no. 10, p. 955–957, https://doi.org/10.1130/0091-7613(2000)28<955:AIROSI>2.0.CO;2.

Nativ, R., and Turowski, J.M., 2020, Site dependence of fluvial incision rate scaling with timescale: Journal of Geophysical Research: Earth Surface, v. 125, https://doi.org/10.1029/2020JF005808.

Ouimet, W.B., Whipple, K.X., and Granger, D.E., 2009, Beyond threshold hillslopes: Channel adjustment to base-level fall in tectonically active mountain ranges: Geology, v. 37, p. 579–582, https://doi.org/10.1130/G30013A.1.

Prokopenko, A.A., Hinnov, L.A., Williams, D.F., and Kuzmin, M.I., 2006, Orbital forcing of continental climate during the Pleistocene: A complete astronomically tuned climatic record from Lake Baikal, SE Siberia: Quaternary Science Reviews, v. 25, p. 3431–3457, https://doi.org/10.1016/j.quascirev.2006.10.002.

Raymo, M.E., 1997, The timing of major climate terminations: Paleoceanography, v. 12, p. 577–585, https://doi.org/10.1029/97PA01169.

Ren, J., Xu, X., Lv, Y., Wang, Q., Li, A., Li, K., Zhu, J., Cai, J., and Liu, S., 2022, Late Quaternary slip rate of the northern Lancangjiang fault zone in eastern Tibet: Seismic hazards for the Sichuan-Tibet Railway and regional tectonic implications: Engineering Geology, v. 306, https://doi.org/10.1016/j.enggeo.2022.106748.

Sadler, P.M., 1981, Sediment accumulation rates and the completeness of stratigraphic sections: The Journal of Geology, v. 89, p. 569–584, https://doi.org/10.1086/628623.

Safran, E.B., Bierman, P.R., Aalto, R., Dunne, T., Whipple, K.X., and Caffee, M., 2005, Erosion rates driven by channel network incision in the Bolivian Andes: Earth Surface Processes and Landforms, v. 30, p. 1007–1024, https://doi.org/10.1002/esp.1259.

Schumer, R., and Jerolmack, D.J., 2009, Real and apparent changes in sediment deposition rates through time: Journal of Geophysical Research, v. 114, F00A06, https://doi.org/10.1029/2009JF001266.

Snyder, N.P., Whipple, K.X., Tucker, G.E., and Merritts, D.J., 2000, Landscape response to tectonic forcing—Digital elevation model analysis of stream profiles in the Mendocino triple junction region, northern California: Geological Society of America Bulletin, v. 112, p. 1250–1263, https://doi.org/10.1130/0016-7606(2000)112<1250:LRTTFD>2.0.CO;2.

Spratt, R.M., and Lisiecki, L.E., 2016, A late Pleistocene sea level stack: Climate of the Past Discussions, v. 12, p. 1079–1092, https://doi.org/10.5194/cp-12-1079-2016.

Val, P., Venerdini, A.L., Ouimet, W., Alvarado, P., and Hoke, G.D., 2018, Tectonic control of erosion in the southern Central Andes: Earth and Planetary Science Letters, v. 482, p. 160–170, https://doi.org/10.1016/j.epsl.2017.11.004.

Wang, Y., Cheng, H., Edwards, R.L., Kong, X., Shao, X., Chen, S., Wu, J., Jiang, X., Wang, X., and An, Z., 2008, Millennial- and orbital-scale changes in the East Asian monsoon over the past 224,000 years: Nature, v. 451, p. 1090–1093, https://doi.org/10.1038/nature06692.

Zhang, J., Yang, H., Liu-Zeng, J., Ge, Y., Wang, W., Yao, W., and Xu, S., 2021, Reconstructing the incision of the Lancang River (Upper Mekong) in southeastern Tibet below its prominent knickzone using fluvial terraces and transient tributary profiles: Geomorphology, v. 376, https://doi.org/10.1016/j.geomorph.2020.107551.

Printed in the USA